Experimental Investigation and Optimization of Laser Cutting Parameters for Solar Cells Based On Taguchi Method

Article · March 2018

DOI: 10.9790/1684-1405024151

3 authors, including:

Alphonse Niyibizi
Dedan Kimathi University of Technology
6 PUBLICATIONS **1** CITATION

SEE PROFILE

IOSR Journal of Mechanical and Civil Engineering (IOSR-JMCE)
e-ISSN: 2278-1684,p-ISSN: 2320-334X, Volume 14, Issue 5 Ver. II (Sep. - Oct. 2017), PP 41-51
www.iosrjournals.org

Experimental Investigation and Optimization of Laser Cutting Parameters for Solar Cells Based On Taguchi Method.

Benson K. Mbithi[a]*, Jean B. Byiringiro[a]. Alphonse Niyibizi[b]
[a*]*School of Engineering, Dedan Kimathi University of Technology, P.O Box 657-10100, Nyeri-Kenya*
[a]*School of Engineering, Dedan Kimathi University of Technology, P.O Box 657-10100, Nyeri-Kenya*
[b]*School of Science, Dedan Kimathi University of Technology, Nyeri-Kenya*
[*]*Corresponding author's email: bensonkilosh@gmail.com*

Abstract*: In recent times, the use of laser has gained popularity in micro machining applications due to the unique properties of the laser beam. Laser micromachining is used in the machining of a wide variety of materials including solar cells. However, this process faces challenges such as microcracking which can be as a result of incorrect combination of laser process parameters. The cutting process requires an optimal combination of cutting parameters which lead to excellent cut quality and quality solar cells. Indeed, the effects of each particular cutting parameter on the output parameters have not been well established for this process. This research is focused on investigating and optimizing the laser beam and process parameters on cut quality attributes of solar cells. The variables which were selected as input parameters are: the scan speed (v), the spot diameter (d), and the laser power (P). The output parameters, quality attributes or responses investigated were: the kerf depth (K.d), the kerf width (K.w), and the material removal rate (MRR). A Taguchi orthogonal array based on Minitab17 software was used for the design of the experiments, analysis, and optimization. The input variables were found to have a significant effect on the quality attributes of the solar cell. The kerf depth was found to increase with the laser power and decreased with the spot diameter and the scan speed. The kerf width was found to increase with the laser power and the spot diameter while it decreased with the scan speed. On the other hand, the material removal rate was found to increase with the laser power and the spot diameter while the scan speed had the opposite effect.*

The optimal conditions obtained for cutting a standard 156mmX156mm solar cell were: the laser power at 126.67W, the spot diameter at 0.4158mm and the scan speed at 3121mm/min. Validation experiments were conducted, and experimental output values obtained were: the kerf depth at 0.1839mm, the kerf width at 0.5828mm and the material removal rate at 1456mm^3/min. These experimental results showed conformity to the optimal conditions obtained using the software.

Keywords: *Laser, Taguchi, Variables, Optimization, Solar cell*

Date of Submission: 19-07-2017 Date of acceptance: 23-09-2017

I. INTRODUCTION

World wide growth of photovoltaics has fit an exponential curve for more than two decades. During this period, solar PV has developed from a small scale source of electricity to become a mainstream electricity source [1]. Parallel to this growth, laser machining has found many applications in silicon processing for the manufacture of different Micro-Electro-Mechanical Systems (MEMS) and Micro Opto-Electro-Mechanical Systems (MOEMS) [2]. This machining process has been preferred because of the key properties in the machining process. These key properties include large absorptance of laser beam energy by silicon and its low convection heat transfer coefficient [3]. Customized solar panels are a new trend which is employed in developing countries designed to provide solar panels for customer specifications. This requires the need to reduce the solar cells in various sizes using laser technology because of its uniqueness in machining [4]. Research has not fully exhausted the optimization of solar cell cutting variables using laser beam processing. Laser cutting process has a demerit of generating heat on the surface of the workpiece which may lead to thermal stresses and developing undesirable cracks [5]. This requires proper and optimal conditions which shall lead to machining with reduced waste heat generation and the adverse effects on the surface of the work piece [6].

The optimization of the cutting variables however requires an efficient statistical method which is able to analyze the responses with the effects and perform the general optimization process for the process. Considerable research studies have been carried out to analyze, simulate and optimize the laser cutting process. Different methodologies were employed for modeling the laser cutting process such as analytical methods, multiple regression analysis (MRA), response surface methodology (RSM), fuzzy expert systems, and artificial

neural networks (ANNs) [7]. Subsequently, the near optimal laser processing conditions were identified by applying classical optimization algorithms or metauristic algorithms like genetic algorithms, simulated annealing and particle swarm optimization [8]. These methods are powerful tools for systematic modeling, analysis and optimization. However, they are time and computationally expensive and require a considerable knowledge in mathematical modeling, optimization theory, statistics and artificial intelligence [9].

On the other hand, the application of the Taguchi method without formulation of any kind of model is an attractive alternative for determining near optimal cutting parameter settings in laser cutting and it is being increasingly applied [10]. The method has proved to be efficient, yet relatively simple and has become particularly popular when dealing with multiple performance characteristics. By using the Taguchi technique, industries are able to greatly reduce product development cycle time for both design and production and thus reducing costs and increasing profit [10].

Sandeep et al. [11] investigated the impact of process parameters like cutting speed, pulse repetition rate (PRR), and shield gas pressure, surface roughness (Ra) of steel (AISI 321 stainless steel) material on laser cutting machining. A L9 orthogonal array was generated for fractional factorial design (Taguchi analysis) for better understanding of the interaction among the process parameters. The values of surface roughness for steel were calculated by regression model equations, and Taguchi Analysis and Genetic Algorithm were used for the parametric analysis of the experimental data. Taguchi analysis gives the optimum values of surface roughness and kerf taper, which are 2.2981 μm and 0.1637° respectively. Genetic algorithm was used for providing a set of optimum values for both outputs simultaneously.

Begic et al. [12] analyzed the effect of the process parameters on the laser cut quality of a tungsten alloy sheet with a thickness of 1 mm. The experiments were conducted at three levels of the selected process parameters such as assist gas type (oxygen, air, and nitrogen) and assist gas pressure. Taguchi design of experiments was used to obtain the optimum conditions through the study of the signal to noise ratio for three quality characteristics such as kerf width, heat affected zone, and surface roughness. Results of this study indicated that the optimal assist gas pressure is entirely different for kerf width, heat affected zone, and surface roughness. The nitrogen was found to be the optimal assist gas for all of three quality characteristics.

Mulembo et al. [1] investigated the thermal effects optimization of Nd: YAG laser beam and process parameters for quality micromachining of monocrystalline silicon. A model for predicting the optimal laser beam and laser process parameters for quality machining of silicon wafers was successfully developed. This study concluded that the laser beam and process parameters have adverse effects on the quality attributes of the monocrystalline silicon. A model for predicting the optimal laser scan speed for quality machining of silicon wafers was developed. The temperature distributions were evaluated using Finite Element Method. The mathematical equations for the simulation model were coded in the COMSOL software, and the result images analyzed using IMAGEJ 103 software. The results indicate that slow scan speeds result to melting and ablation in silicon. Slow speeds are optimal for applications such as drilling holes, and trepanning of silicon wafers. On the other hand, high scan speeds result in minimal melting. High speeds are optimal for annealing , surface modification and texturization applications on monocrystalline silicon. Cutting quality is improved if scan speeds of the laser are chosen properly.

II. MATERIALS AND METHODS

2.1 Materials and equipment used

In this research, p-type monocrystalline silicon solar cells were used as the workpiece. They had a dimension of 156mm by 156mm by 200μm. Such solar cells have 3 busbars on the front side and 3 busbars at the back side as shown in Fig.1.

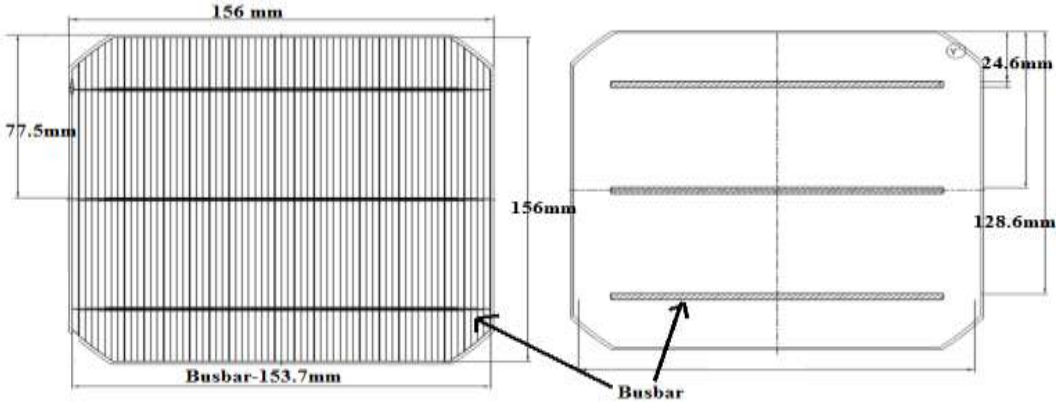

Fig. 1: Features of the monocrystalline P-type solar cell

2.2 Laser engraving and cutting machine

Laser engraving machine HZE-12080 (Fig. 2) was used for cutting the solar cells using the specified parameters. The machine is equipped with CO2 laser tube and can be used to cut and engrave on wood, bamboo, Plexiglas, crystal, leather, rubber, marble, ceramics, and glass, etc. It has a power range of 80W-150W, cutting speeds of 0-36000mm/s [13], and spot diameter of 0.12-0.6mm. It supports multiple graphic formats, such as HPGL, BMP, GIF, JPG, JPEG, DXF, and DST. It features DSP Control System for RDdraw, CoreDraw and AutoCAD and other advanced design software.

Fig. 2: Laser cutting machine (HZE-12080)

2.3 P879 Depth scope

The P879 Depth scope shown in Fig. 3 was used for measurement of the kerf width and depth. The P879 is a portable microscope for measuring depth/thickness and size of objects. It has a vernier combined with a microscope and a calibrated scale which is used to measure the required dimension.It has a magnification of x2000 approximately [14].

Fig. 3: P879 Depthscope

2.4 Taguchi design of experiments

Taguchi design method is also referred to as experimental design "off-line quality control" because it is a method of ensuring good performance in the design stage of products or processes [10]. Taguchi 9-orthogonal array was used to design the experiments to be conducted. The parameters were set to their low, medium and high levels according to the limits of the laser machine. Table 1 below shows the orthogonal array design which was used.

Table 1: Orthogonal array design

Parameter	Low level	Medium level	High level
Laser power (W)	80	115	150
Spot diameter (mm)	0.12	0.36	0.6
Scan speed (mm/min)	3000	5000	7000

Once these levels were set in Minitab software, table 2 was generated which shows the design of experiments to be conducted.

Table 2: Taguchi design of experiments

P (W)	d(mm)	v(mm/min)
80	0.12	3000
80	0.36	5000
80	0.6	7000
115	0.12	5000
115	0.36	7000
115	0.6	3000
150	0.12	7000
150	0.36	3000
150	0.6	5000

These parameters were set while performing the machining of solar cell using HZE-12080 laser machine as shown in the experimental set-up in Fig. 4 below.

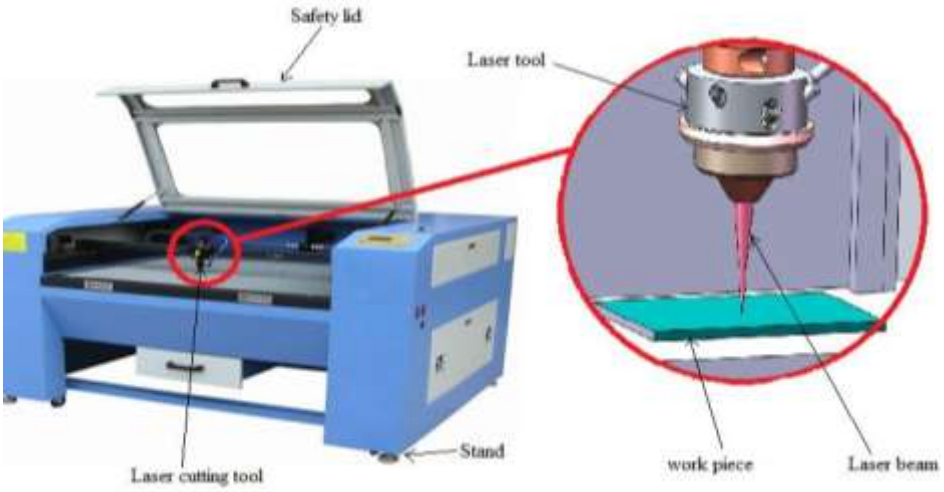

Figure 4: Experimental set-up

III. RESULTS AND DISCUSSION

After performing the experiments as by the Taguchi design, the parameters values were tabulated as shown in Table 3. The kerf depth, kerf width and the material removal rate were measured and recorded against the input combinations for each experiment.

Table 3: Results tabulation

P(W)	d(mm)	v(mm/min)	K.d (mm)	K.w (mm)	MRR(mm^3/min)
80	0.12	3000	0.1851	0.6458	1252.08
80	0.36	5000	0.1787	0.6354	1375.51
80	0.6	7000	0.1709	0.6784	1500.31
115	0.12	5000	0.1844	0.5894	1201.71
115	0.36	7000	0.1770	0.5729	1324.43
115	0.6	3000	0.1808	0.6201	1591.58
150	0.12	7000	0.1841	0.5865	1147.26
150	0.36	3000	0.1859	0.5986	1423.56
150	0.6	5000	0.1786	0.6258	1546.79

3.1 Discussion of the results

After performing the experiments, the data set was analyzed for the main effects of the factors on the responses and the analysis of variance (ANOVA) were also performed with a risk level of 0.05, using individual responses. The input variables and output responses in the results table were analyzed at high accuracy (R-squared adjusted of 98.72%, 99.16%, and 99.97% for kerf depth, kerf width and material removal rate respectively). The Taguchi design method advises to utilize P-value displayed in the ANOVA tables of results as a reference for the investigation of parameter effects in the model development (the P value is often set to 0.01 or 0.05).

In this study, Minitab statistical software (version 17) was used to evaluate the correlation between input variables and the responses. This analysis considers the laser power as the input A, the spot diameter as the input B, and the scan speed as the input parameter C.

i. Kerf depth

Main effects analysis for kerf depth

The plot in Fig. 5 shows that the laser power of 150W was associated with the highest mean strength of 0.1828mm for kerf depth with 80W being associated with the lowest mean strength of 0.1782mm. The plot shows that with increasing laser power, the kerf depth was found to increase to a maximum value of 0.1828mm. For the spot diameter, a laser beam diameter of 0.12mm had the highest mean strength of 0.1846mm while the diameter of 0.6mm had the lowest effect of 0.1764mm. The plot shows that with increasing spot diameter the kerf depth decreases. For the scan speed, the level of 3000mm/min had the highest mean strength of 0.1837mm while the maximum level of 7000mm/min had the lowest effect of 0.1773mm. In general the kerf depth was found to decrease with increasing scanning speed of the laser beam.

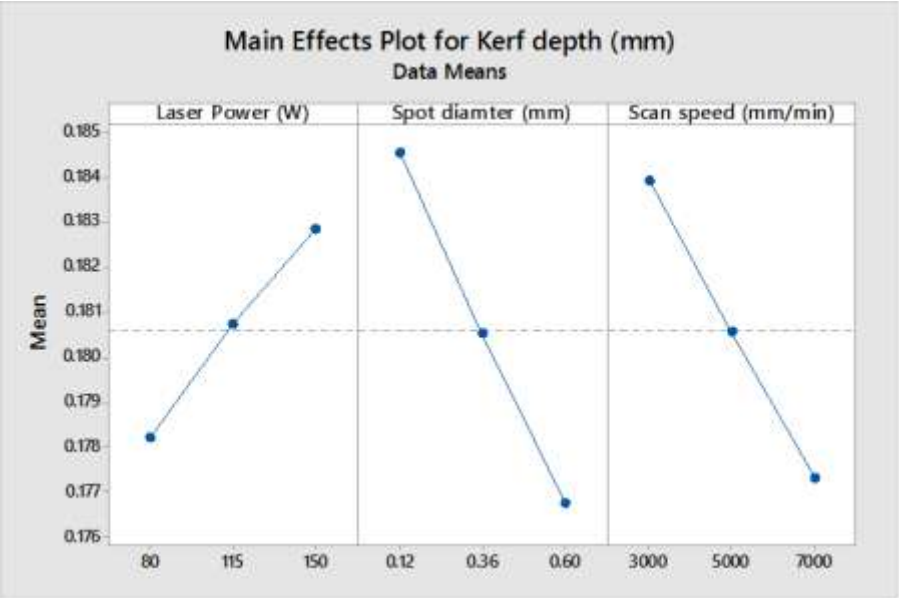

Fig. 5: Main effect plot for Kerf depth

ANOVA for kerf depth

As shown in the ANOVA Table 4 for kerf depth, the impacts of factors A, B, AC, AA, and BB were more significant because the P-value is less than the risk value of 0.05.

The P-value for factor C and interaction factors CC were 0.117 and 0.089 respectively, which were close to the risk level (0.05). Therefore, they should also be included in the final model of kerf depth as shown in the equation (1):

$$K.d = 0.1849 + 0.000085A + 0.002262B - 0.000002C - 0.0000001A^2 - 0.004919B^2 - 0.00000013C^2 + 0.000001AC \quad (1)$$

Table 4: ANOVA table for kerf depth

Sourceof variation	DOF	AdjSS	Adj MS	F-value	P-Value
Regression	6	0.000190	0.000032	1345.72	0.001
A	1	0.000001	0.000001	61.62	0.006
B	1	0.0000002	0.0000002	11.11	0.050
C	1	0.000001	0.0000001	23.82	0.117
AB	1	0.0000003	0.0000002	5.84	0.270
AC	1	0.0000002	0.0000001	2.28	0.059
BC	1	0.0000001	0.0000000	15.42	0.367
AA	1	0.0000002	0.000000	927.82	0.012
BB	1	0.0000001	0.000001	19.09	0.031
CC	1	0.000001	0.0000001	9.09	0.089
Error	2	0.000001	0.000001		
Total	11	0.000190			

ii. Kerf width

Main effects analysis for kerf width

For laser power as seen in Fig. 6, the level of 80W was associated with the highest mean strength of 0.6541mm with 115W having the lowest mean effect of 0.5934mm. The plot shows that kerf width decreases with increasing laser power from 80W to 115W and then starts to increase with increasing power to 150W. For the spot diameter, the level of 0.6mm was associated with the highest mean strength of 0.6449mm and spot diameter of 0.36mm was associated with the lowest mean strength of 0.6026mm. In general, the kerf width was found to decrease with increasing spot diameter from 0.12mm to 0.36mm and started to increase with increasing spot diameter further to 0.6mm. Scan speed of 3000mm was associated with the highest mean strength of 0.6231mm while a speed of 7000mm/min was associated with the lowest effect of 0.6121mm of kerf width. In general the kerf width was found to decrease with increasing scan speed.

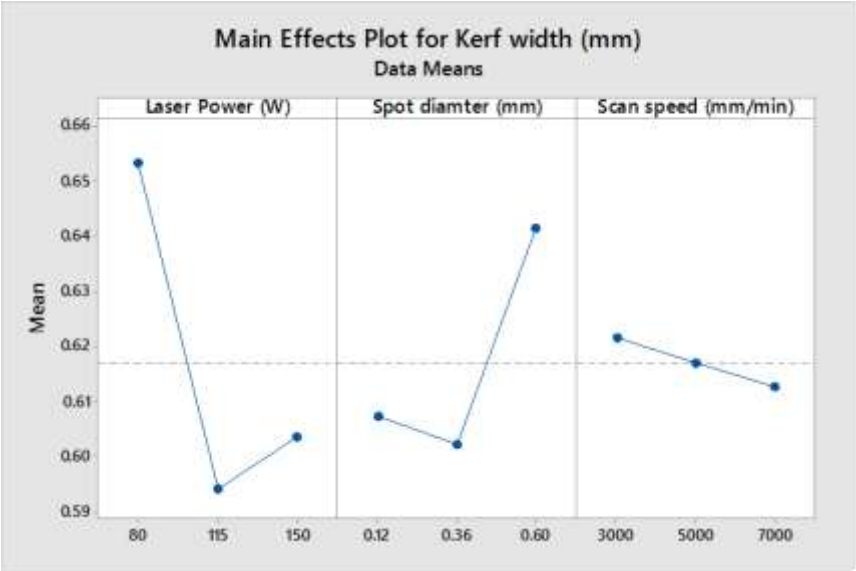

Fig. 6: Main effect plot for Kerf width

ANOVA for kerf width

As shown in Table 5 factors A, B, and interaction factor AA have P-values less than 0.05 hence they are the most significant to the kerf width. Factor C and interaction factors BC and AC have P- values of 0.059, 0.072 and 0.056 respectively which are close to the risk value hence they should also be included in the model for kerf width as seen in equation (2).

$$K.w = 1.018 - 0.0066A - 0.2834B - 0.00001C - 0.000028A^2 - 0.000099BC - 0.0000001AC \quad (2)$$

Table 5: ANOVA table for kerf width

Sourceof variation	DOF	AdjSS	Adj MS	F-value	P-Value
Regression	7	0.009000	0.001286	2380.91	0.016
A	1	0.002140	0.002140	3963.29	0.020
B	1	0.000281	0.000281	520.08	0.018
C	1	0.002351	0.002351	114.52	0.059
AB	1	0.001032	0.001032	1.05	0.492
AC	1	0.001562	0.001562	188.84	0.056
BC	1	0.000021	0.000021	172.42	0.072
AA	1	0.000102	0.000102	4353.14	0.010
BB	1	0.000372	0.000372	1911.25	0.178
CC	1	0.000167	0.000167	1828.98	0.198
Error	2	0.000001	0.000001		
Total	11	0.017029			

iii. Material removal rate

Main effect analysis for the material removal rate

As we can see in Fig. 7, for the laser power, the level of 150W was associated with the highest mean strength of 1454mm^3/min while the laser power of 80W was associated with the lowest mean strength of 1260mm^3/min. The material removal rate was found to increase as the laser power was increased from 80W to 150W. The spot diameter of 0.6mm was associated with the highest mean strength of 1547 mm^3/min while a diameter of 0.12 was associated with the lowest effect of 1201 mm^3/min. The material removal rate was found to increase with increasing spot diameter. For the scan speed, the level of 3000mm/min was associated with the highest mean strength of 1412 mm^3/min while a speed of 7000mm/min was associated with the lowest effect of 1311 mm^3/min. The plot showed that the material removal rate decreased as the scan speed was increased from 3000mm/min to 7000mm/min.

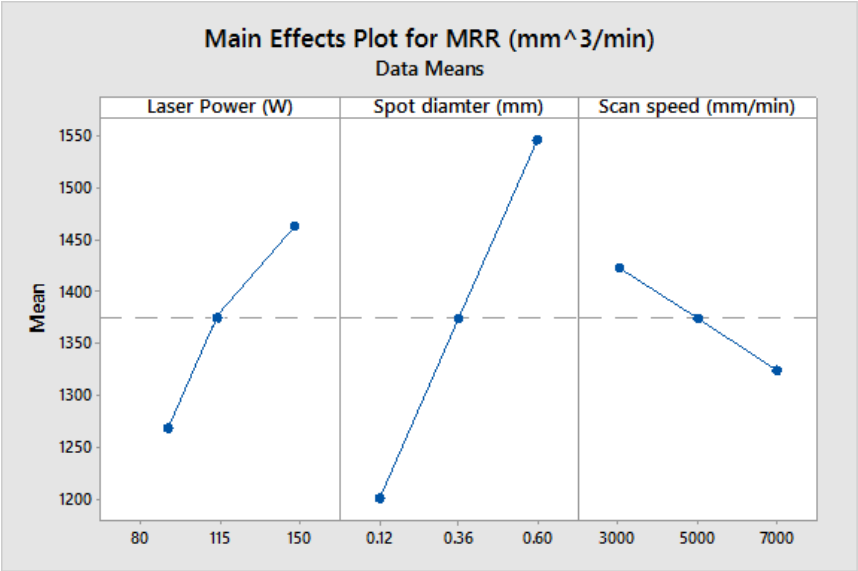

Fig.7: Main effect plot for material removal rate

ANOVA for material removal rate

From the ANOVA Table 6, the factors A, B, and interaction factors BC and C^2 have P-values less than the risk value. This means they are the most significant factors to influence the material removal rate for the process.

Factor C and interaction factors $A^2$and AC have p-values 0.075, 0.061 and 0.051 respectively which were near the risk value of 0.05 and hence they were included in the equation too.
The model relating the material removal rate and the factors is given in equation (3).

$$MRR = 1244 - 0.2246A + 663.7B - 0.01777C + 0.001370A^2 + 0.0000001C^2 - 0.000053AC + 0.000012BC \quad (3)$$

Table 6: ANOVA table for material removal rate

Sourceof variation	DOF	AdjSS	Adj MS	F-value	P-Value
Regression	8	194026	24253.2	28769.34	0.005
A	1	2	2.5	0.08	0.022
B	1	1342	1341.6	1906.03	0.075
C	1	70	69.6	272.37	0.089
AB	1	13	13.4	0.31	0.678
AC	1	21	21.0	2.67	0.051
BC	1	17	17.3	0.19	0.028
AA	1	6	5.6	0.05	0.061
BB	1	1	0.7	0.01	0.925
CC	1	0	0.0	0.02	0.013
Error	2				
Total	11				

b. Optimization process

For optimization, each response variable has its own criteria used to optimize. Minitab software has an in-built optimization process which performs the calculations and provides the optimized values.

i. Kerf depth

Since the depth of cut determines the machining time and the amount of cut material in a given time, it was chosen to be nominal. This is because having it so deep would make the process inefficient because much power would be spent for cutting a sample which would require less power. Following this, a target of 0.184 mm was set for the kerf depth which was suitable for the cutting process of the solar cell.

ii. Kerf width

The more the kerf width, the more material is wasted and also the more the time to machine is required. Therefore the more power is used in the process. The kerf width should be minimum. Hence this research put minimum kerf width as the best criterion.

iii. Material removal rate (MRR)

Maximum material removal rate dictates how efficient and profitable the production is. Having a low material removal rate incurs the concerned industry high costs in production since the machining time is increased. This is why the material removal rate needs to be high. Hence the material removal rate was set to the maximum value (larger is better) for the optimization process.

iv. Response Optimization: kerf depth, kerf width, MRR

The section below covers the solution of the optimization process. Table 7 shows the parameter values which were used in the optimization process. As previously discussed, the kerf depth was set to a target value of 1.840mm, the kerf width was set to the minimum and the MRR was set to the maximum.

Table 7: Parameters used

Response	Goal	Lower	Target	Upper	Weight	Importance
K.d(mm)	Target	0.17	0.184	0.1859	1	1
K.w(mm)	Minimum		0.57	0.6784	1	1
MRR(mm^3/min)	Maximum	1147.26	1591.58		1	1

The variable ranges which were used in the designing of the experiment by Taguchi method are as shown in Table 8.

Table 8: Variable ranges

Variable	Values
Laser power (W)	(80, 150)
Spot diameter (mm)	(0.12, 0.6)
Scan speed (mm/min)	(3000, 7000)

The solution for the response optimization providing the optimal conditions and the predicted optimum response factors are shown in Table 9 below.

Table 9: Solution for Multiple Response Prediction (optimized variables)

P(W)	D (mm)	v (mm/min)	MRR (mm^3/min)	K.w (mm)	K.d (mm)	Composite desirability
			Fit	Fit	Fit	
126.6667	0.4158	3121.2121	1457.76	0.583252	0.1840	0.857114

The optimal conditions are: 126.6667W, 0.4158mm, and 3121.2121mm/min for laser power, spot diameter and scan speed respectively. The predicted response factors are: 0.857114mm, 0.583252mm, and 1457.76mm^3/min for kerf depth, kerf width and MRR, respectively. The optimization plot is shown in Fig. 8 below.

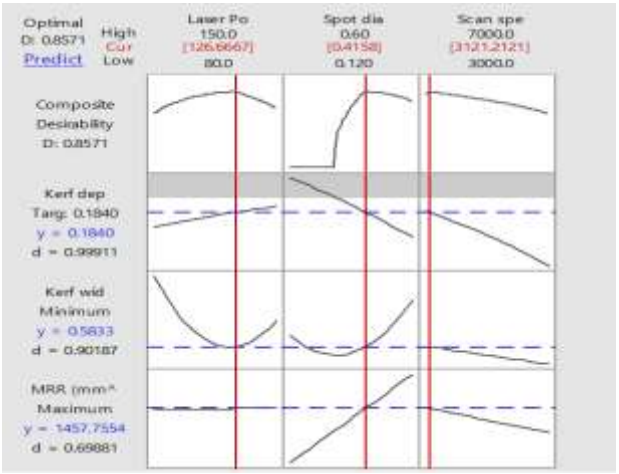

Fig. 8: Minitab optimization plot

The optimized response variables are shown in Table 10 below. The fit, standard error fit, the 95% confidence interval and 95% prediction intervals are shown as ranges for each response variable.

Table 10: Optimized response variables

Response	Fit	SE Fit	95%CI	95%PI
K.d(mm)	0.1840	0.0012	(0.18086, 0.18714)	(0.17817, 0.18983)
K.w (mm)	0.583252	0.000629	(0.575255, 0.591250)	(0.570959, 0.595546)
MRR (mm^3/min)	1457.76	0.03	(1457.42, 1458.09)	(1457.24, 1458.27)

Table 11 shows the values of the factors required to obtain the optimal responses

Table 11: Optimal factors

Variable	Setting
Laser power (W)	126.6667
Spot diameter (mm)	0.4158
Scan speed (mm/min)	3121.2121

c. Validation of the values

After setting these variables, the experiment was repeated again for 3 times to validate the optimization and the following values were obtained for the response variable.

i. Experimental results for validation

Table 12 shows the experimental results for the validation of these optimal conditions as performed on the same machine and work piece.

Table 12: Experimental validation

Run	**Kerf depth (mm)**	**Kerf width(mm)**	**MRR**
1	0.1836	0.5825	1455
2	0.1839	0.5830	1459
3	0.1842	0.5828	1454
Mean	0.1839	0.5828	1456
Standard deviation	1E-04	0.0005	1.76

ii. Comparison of experimental response factors with predicted values

The predicted and the experimental values for the response factors were tabulated in Table 13 for comparison.

Table 13: Predicted values and experimental values for responses

Response factor	**Kerf depth (mm)**	**Kerf width(mm)**	**MRR(mm^3/min)**
Predicted value	0.1840	0.583252	1457.76
Experiment 1	0.1836	0.5828	1455
Experiment 2	0.1839	0.5835	1459
Experiment 3	0.1842	0.5830	1454

Predicted versus experimental values for kerf depth

As seen in Fig. 9, the predicted kerf depth is conforming to the experimental kerf depth with a slight variation in the graph. This graph validates the developed model for the kerf depth as in equation (1) and hence can be used in future kerf depth estimation given the input parameter values.

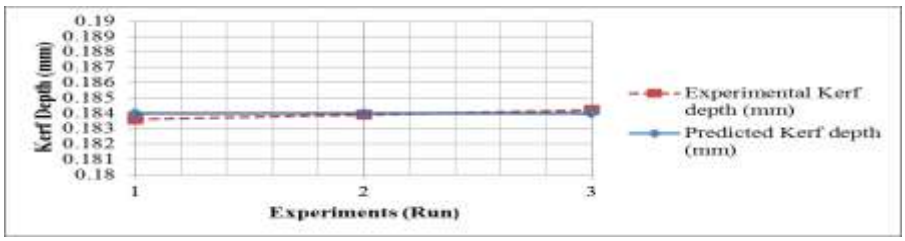

Figure 9: Graph of predicted and experimental values for kerf depth

Predicted versus experimental values for kerf width

The graph in Fig.10 shows the conformity of the experimental values obtained for the kerf width and the predicted values. The graph validates the model in that there is a slight variation in the two linear graphs. This means that the model developed for kerf width in equation (2) is applicable when estimating the kerf width for laser cutting of solar cells given the input parameters considered in this research.

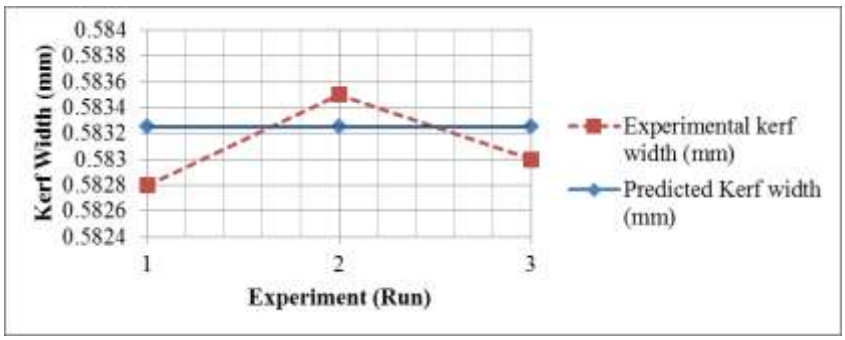

Figure 10: Graph of predicted and experimental values for kerf width

Predicted versus experimental values for MRR

The graph in Fig.11 of predicted values and experimental values for MRR shows conformity with a slight variation. This means that the model developed for the MRR in equation (3) is valid and can be used in estimating the material removal rate for laser cutting of solar cells. From the obtained data, it can be seen that the mean of the kerf depth, 0.1839mm is within the range given by the predicted values by the optimization due to the small standard deviation of 1E-04 from the mean. The kerf width mean was 0.5828mm with a standard deviation of 0.0005, which is also within the acceptable range given by the prediction. The same case applies to MRR; the average was 1456mm^3/min with a standard deviation of 1.76, which is still within the predicted range.

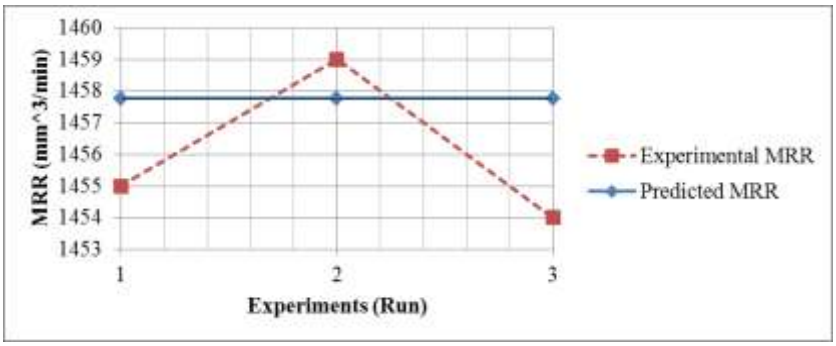

Figure 11: Graph of predicted and experimental values for MRR

This analysis shows that the model developed from the experiments for optimization was valid and the factor values for optimal responses were determined.

IV. CONCLUSION

This research investigated the effects of input process parameters over the response parameters for laser cutting of solar cells. The response parameters were then recorded and the effect of each of the input variables was investigated. The optimization process was done with the aid of Minitab optimization tool which has provided the optimized values for the three input parameters (laser power, scan speed and spot diameter). Finally a validation experiment was done to verify the predicted response variables by the Optimization tool. The response variables' values obtained after the experiment were hence close to the predicted response variables by the Minitab Optimizer tool.

Acknowledgements

Our special acknowledgement goes to African Development Bank in collaboration with Dedan Kimathi University of Technology for the grant of the scholarship which made this research a success. Our acknoledgement also goes to Ubbink Eastern Africa Ltd for the opportunity to use their industrial laser equipment and materials for the experimental part of the research.

REFERENCES

[1] Titus Mulembo, James keraita, B. Ikua. "Numerical Study of Scan Speed Selection and Kerf Depth prediction in silicon laser machining." *The International Institute for Science, Technology and Education (IISTE)* (2015): 3-8.

[2] Osellame, R.,Cerullo, G., & Ramponi, R. *Femtosecond laser micromachining: photonic and microfluidic devices in transparent materials*. Springer Science & Business Media, 2012.

[3] Madić, Miloš. "Comparative modeling of CO2 laser cutting using multiple regression analysis and artificial neural network." *International Journal of Physical Sciences* (2012): 3-9.

[4] Wang, Qi K. "A study on the laser marking process of stainless steel." *Journal of Materials Processing Technology* (2003): 273-276.

[5] Araújo, D. "Microstructural study of CO2 laser machined heat affected zone of 2024 aluminium alloy." *Applied surface science*. 2009. 210-217.

[6] Lamikiz, A. "CO2 laser cutting of advanced high strength steels (AHSS)." *Applied surface science* 2010: 362-368.

[7] Hrelja, M. "Particle swarm optimization approach for modelling a turning process." *Advances in Production Engineering & Management* (2014): 3-10.

[8] Michalski, R. *Machine learning: An artificial intelligence approach*. Springer Science & Business Media., 2013.

[9] Bhaduria, O. S. "Application of Taguchi method for optimization of process parameters for minimum surface roughness in turning of 45c8." *Futuristic Trends in Engineering, Science, Humanities, and Technology FTESHT* (2016): 13-18.

[10] Chen, W. C. "Optimization of the plastic injection molding process using the Taguchi method, RSM, and hybrid GA-PSO." *he International Journal of Advanced Manufacturing Technology* (2016).

[11] Kumar, Sandeep. "Parametric optimization of cutting parameters of laser assisted cutting using Taguchi analysis and genetic algorithm." *Journal on Future Engineering and Technology* (2016): 36-42.

[12] Begic-Hajdarevic. "Optimization of process parameters for cut quality in CO2 Laser cutting using Taguchi method." *Annals of DAAAM & Proceedings*. 2016. 1-8.

[13] *HZE-12080:laser engraving machine HZE-12080*. n.d. Hanzlaser. 16 June 2016. <http://www.hanzlaser.com/products/laser-engraving-machine/laser-engraving-machine-HZE-12080.htm>.

[14] *Portable depth measuring microscope*. n.d. MPL. 16 June 2016. <http://www.microscopesplus.co.uk/page79a.html>.

Benson K. Mbithi Experimental Investigation and Optimization of Laser Machining Process Parameters for Solar Cell Using Taguchi Method..” IOSR Journal of Mechanical and Civil Engineering (IOSR-JMCE) , vol. 14, no. 5, 2017, pp. 41-51.